

Magnetic anisotropy of disordered Mn-Pt layered surface compounds on Pt(111)

S. Gallego

*Center for Computational Materials Science and Institut für Technische Elektrochemie und Festkörperchemie,
Technische Universität Wien, Getreidemarkt 9, A-1060 Wien, Austria
and LURE, Bâtiment 209D, Centre Universitaire Paris-Sud, 91405 Orsay, France*

M. C. Muñoz

Instituto de Ciencia de Materiales de Madrid, Consejo Superior de Investigaciones Científicas, Cantoblanco, 28049 Madrid, Spain

J. Zabloudil

*Center for Computational Materials Science and Institut für Technische Elektrochemie und Festkörperchemie,
Technische Universität Wien, Getreidemarkt 9, A-1060 Wien, Austria*

L. Szunyogh

*Department of Theoretical Physics, Technical University of Budapest, Budafoki út. 8, 1521 Budapest, Hungary
and Center for Computational Materials Science and Institut für Technische Elektrochemie und Festkörperchemie,
Technische Universität Wien, Getreidemarkt 9, A-1060 Wien, Austria*

P. Weinberger

*Center for Computational Materials Science and Institut für Technische Elektrochemie und Festkörperchemie,
Technische Universität Wien, Getreidemarkt 9, A-1060 Wien, Austria*

(Received 30 May 2000; published 23 January 2001)

The magnetic moments and the anisotropy energy of surface compounds formed by $\text{Mn}_x\text{Pt}_{(1-x)}$ ($x \in [0,1]$) on a Pt(111) substrate are calculated by means of the fully relativistic spin-polarized screened Korringa-Kohn-Rostoker method. The binary compositions are modeled within the coherent potential approximation. Different Mn concentrations at each layer have been considered in order to understand the influence on the magnetic properties of both the chemical environment of the Mn atoms and the segregation of Pt from the bulk. Special emphasis is devoted to the study of the layered sequences $\text{Pt}/\text{Mn}_x\text{Pt}_{(1-x)}$.

DOI: 10.1103/PhysRevB.63.064428

PACS number(s): 75.30.Gw, 75.70.Rf, 75.70.Ak, 75.70.Cn

I. INTRODUCTION

Thin films and multilayers of large perpendicular magnetic anisotropy are widely applied in the design of high-density magnetic and magneto-optical storage devices.¹ The combinations of magnetic and nonmagnetic transition metals are specially suitable to show this property.^{2,3} However, the subtle dependence of the magnetic anisotropy on the structural and compositional parameters makes it difficult to predict general model structures that can be used in the development of future devices. A further complication arises from the stability of low-dimensional systems, as the equilibrium phase diagram can be completely different to that of the bulk.

A layered surface compound made up by alternated planes of Pt and of ordered stoichiometric MnPt_3 composition onto a Pt(111) substrate has been synthesized recently.⁴ Its formation involves segregation processes based on annealing Mn deposits of several monolayers supported on a Pt(111) substrate. Both the alternated sequence and the global stoichiometry are different from any bulk Pt-Mn binary phase. Although the depth that the final (2×2) -Pt/MnPt₃ surface sequence extends into the substrate is not known exactly, a dynamical low-energy electron diffraction analysis indicates that it covers at least the first four layers. The termination in Pt at the topmost plane cannot be explained from

simple thermodynamical arguments regarding the surface tension. On the other hand, this termination seems to reflect a tendency of the Mn atoms to become completely surrounded by nonmagnetic Pt neighbors. The magnetic properties of Mn have been shown to be relevant in the formation of different surface alloys, such as the $(2 \times 2)\text{MnCu}/\text{Cu}(100)$;⁵ not only does the high spin state of Mn determine the stability of this surface alloy, but it is also the driving force for the extremely buckled atomic disposition. In the case of the layered compound, the magnetic character of Mn can also be crucial in the energy balance that leads to the final structure.

In order to investigate this aspect, we have performed *ab initio* calculations of the electronic structure of different Mn-Pt based surface compounds supported on a Pt(111) substrate. Our aim is to determine the variation of the magnetic properties, especially the magnetic anisotropy, depending on the distribution of the Mn atoms in the surface layers. These results can shed light on the origin of the segregation processes leading to the stable (2×2) -[Pt/MnPt₃]/Pt(111) surface. In addition, the structures under study can be considered as ideal candidates for the development of new magneto-optical recording devices. This is not only due to their low dimensionality, but also to the relevant magneto-optical properties of some related bulk structures such as the MnPt₃ compound, which exhibits a high Kerr effect for films grown along (111).⁶

II. COMPUTATIONAL DETAILS

Our calculations are based on the relativistic, spin-polarized screened Korringa-Kohn-Rostoker (SKKR) method⁷ for layered systems.⁸ For each structure considered, the effective potentials and effective exchange fields have been obtained self-consistently using $30\mathbf{k}_{\parallel}$ points in the irreducible wedge of the surface Brillouin zone (ISBZ). Energy integrations were performed along a semicircular contour using a 16-point Gaussian sampling on an asymmetric mesh. The maximum orbital quantum number was set to two. Dipole terms were included in the Madelung constants. Only ferromagnetic configurations of the Mn atoms have been considered in the present paper.

The chemical composition of each layer was modeled within the coherent potential approximation (CPA) for disordered alloy systems.⁹ In this way, only (1×1) unit cells are considered. It has the advantage of reducing the computational effort, which in turn allows us to deal with a wider number of structures. In addition, it enables us to model in a realistic way segregation effects that are involved in the formation of the systems under study, and also in that of the corresponding ordered stoichiometries.

The magnetic anisotropy energy (MAE) has been determined based on the magnetic force theorem.¹⁰ For a given structure, the MAE is defined as

$$\text{MAE} = \Delta E_b + \Delta E_{dd} \quad \Delta E_b = E_b(\parallel) - E_b(\perp)$$

$$\Delta E_{dd} = E_{dd}(\parallel) - E_{dd}(\perp),$$

where ΔE_b and ΔE_{dd} are the band energy and classical magnetic dipole-dipole interaction energy contributions, respectively. The symbols \perp and \parallel refer to the magnetic configurations with the magnetization perpendicular to the surface and parallel to it, respectively. The value of ΔE_{dd} is calculated solving the magnetostatic Poisson equation.¹¹ ΔE_b is obtained by the SKKR method, including $954\mathbf{k}_{\parallel}$ points of the ISBZ. This fine mesh is needed to achieve the precision required to evaluate the MAE. It should be noted that a positive MAE corresponds to a preferential axis of the magnetization pointing along the surface normal.

Three different kinds of surface structures on a Pt(111) substrate have been considered. For all of them, the atomic distances have been set to the ideal values of the fcc Pt lattice; this is in accordance with the experimental values obtained for the layered (2×2) -[Pt/MnPt₃]/Pt(111) compound,⁴ and also with the slight lattice mismatch ($\sim 0.8\%$) between the ordered bulk MnPt₃ alloy and a Pt crystal.¹² First, we have studied systems of global stoichiometry MnPt₃ in up to four overlayers. Second, a Mn_xPt_(1-x) layer, with x ranging from 0 to 1, buried under 3 Pt planes. Finally, we included also in our study surface systems formed either by a variable number of Mn_{0.25}Pt_{0.75} layers, or by an alternating distribution of Pt/Mn_{0.25}Pt_{0.75} planes.

III. RESULTS

A. Four-layer surfaces with MnPt₃ stoichiometry

Our first analysis concerns systems formed by four atomic planes on top of Pt(111), such that the global ratio of Mn/Pt

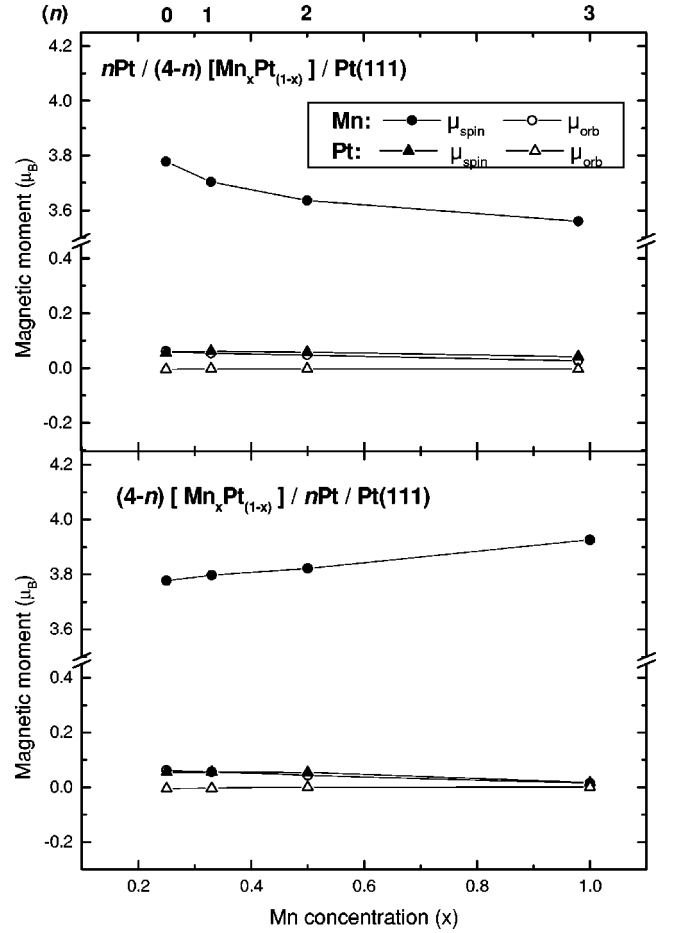


FIG. 1. Mean values of the magnetic moment per atom of the surfaces formed by the four topmost layers of global stoichiometry MnPt₃. Each structure is characterized by the concentration of Mn in the layers of binary composition (x), and the number (n) and location of the pure Pt layers. The upper panel shows Pt-ended surfaces, while the lower one corresponds to structures containing Mn at the outermost plane. The chemically resolved orbital and spin components are shown separately. The same scale has been used for all axes.

atoms in the surface region is $1/3$. Both Pt-terminated surfaces and those having Mn at the topmost plane are considered. For a given structure, we maintain a constant composition in all layers containing Mn; this leads to the following sets of four-layer surfaces: $4[\text{Mn}_{0.25}\text{Pt}_{0.75}]$, $\text{Pt}/3[\text{Mn}_{0.33}\text{Pt}_{0.67}]$, $2\text{Pt}/2[\text{Mn}_{0.50}\text{Pt}_{0.50}]$, and $3\text{Pt}/\text{Mn}$, the pure Pt layers being located at the interface either with the vacuum or with the substrate. The constant chemical ratio at the surface region allows us to compare directly the total energy of all these structures. Although no convergency with respect to the number of \mathbf{k}_{\parallel} points has been investigated, our results indicate that a topmost layer of pure Pt lowers the energy of the system. This is particularly true when we compare the two $3\text{Pt}/\text{Mn}$ structures; then, the largest reduction of energy of the whole set is obtained by the termination in Pt.

In Fig. 1, we show the mean values of the magnetic moments with respect to the top four layers,

TABLE I. Layer by layer evolution of the Mn spin moments (in μ_B) for four-layer surfaces of global stoichiometry MnPt_3 . Each structure is characterized by the concentration of Mn (x) at those planes with nonpure Pt content. The layers are numbered from the topmost plane (**layer 1**) to the bulk (**layer 4**).

| Structure | $x=1.00$ | $x=0.50$ | $x=0.33$ | $x=0.25$ | $x=0.33$ | $x=0.50$ | $x=0.98$ |
|-----------|----------|----------|----------|----------|----------|----------|----------|
| Layer 1 | 3.93 | 3.93 | 3.98 | 3.99 | | | |
| Layer 2 | | 3.71 | 3.71 | 3.74 | 3.79 | | |
| Layer 3 | | | 3.70 | 3.67 | 3.63 | 3.63 | |
| Layer 4 | | | | 3.71 | 3.69 | 3.64 | 3.56 |

$$m_s^\alpha = \frac{1}{N^\alpha} \sum_i m_s^{i,\alpha}, \quad (1)$$

where i runs over all those planes containing the element considered, α indicates the component (Mn or Pt), and s specifies the type of magnetic moment (spin or orbital). N^α serves to normalize to the actual number of layers included in the sum; as an example, $N=4-n$ for $\alpha=\text{Mn}$. The two panels of the figure refer to different terminations, the case $x=0.25$ being common to both. The largest variations between structures correspond to the dominant Mn spin moment, which increases uniformly as more Mn atoms are present in the topmost planes. This is due to the enhancement of the layer-resolved Mn spin moment at the surface, as seen in Table I. We also observe from this table that, for a given layer, higher values correspond to the systems with lower concentrations of Mn ($x < 0.50$). This reflects a tendency of the Mn atoms to enlarge their spin moment when reducing the number of magnetic neighbors.

The total values of the MAE are depicted in Fig. 2. Their variation is governed mostly by the band energy part coming from the Pt atoms. We find the only negative MAE, that is, a favored in-plane magnetization direction, for a pure Mn layer covering a Pt substrate; this behavior has been observed previously in different transition metal structures.^{13,14} As this surface has the highest total energy, it can be concluded that a stable binary Mn-Pt/Pt(111) surface system has a preferred magnetization direction along the (111) axis.

B. Buried $\text{Mn}_x\text{Pt}_{(1-x)}$ layer

To isolate the effect of the in-plane environment of the magnetic atoms, we have studied surfaces containing a single $\text{Mn}_x\text{Pt}_{(1-x)}$ layer capped by 3 Pt planes. In the upper graph of Fig. 3 we give the dependence on x of the chemically resolved magnetic moments at the alloyed layer. As a reference, we have also depicted the moments of the lower adjacent Pt plane, the contribution from the upper one being very similar. Together with the results of the previous section, this figure proves that the Mn atoms have higher magnetic moments when surrounded by fewer Mn neighbors, either in the same plane or in adjacent ones. This is in agreement with the observed evolution of the magnetic moments of Mn in different bulk structures (for example, the moment of a Mn impurity in a nonmagnetic host is larger than that of an atom in a Mn crystal).

This dependence on the number of magnetic neighbors is also reflected in the anisotropy energy. In the lower graph of

Fig. 3 we show the total MAE of the $3\text{Pt}/\text{Mn}_x\text{Pt}_{(1-x)}$ surface, and its decomposition into ΔE_b and ΔE_{dd} . The $\Delta E_b(\text{Mn})$ clearly goes up to $x=67\%$, beyond which it gradually decreases. This reduction for higher Mn concentrations seems to be associated to the magnetic character of the Mn first neighbors. Note that in the present case of a Mn monolayer buried with 3 Pt layers, this tendency is much less prominent than in the previous case of a Mn-rich surface layer (see the lower panel of Fig. 2). The inflection at 67% of Mn is not seen in the Pt contribution, which dominates the MAE. As the MAE is always positive, our results show that the (111) direction is the preferential orientation of magnetization.

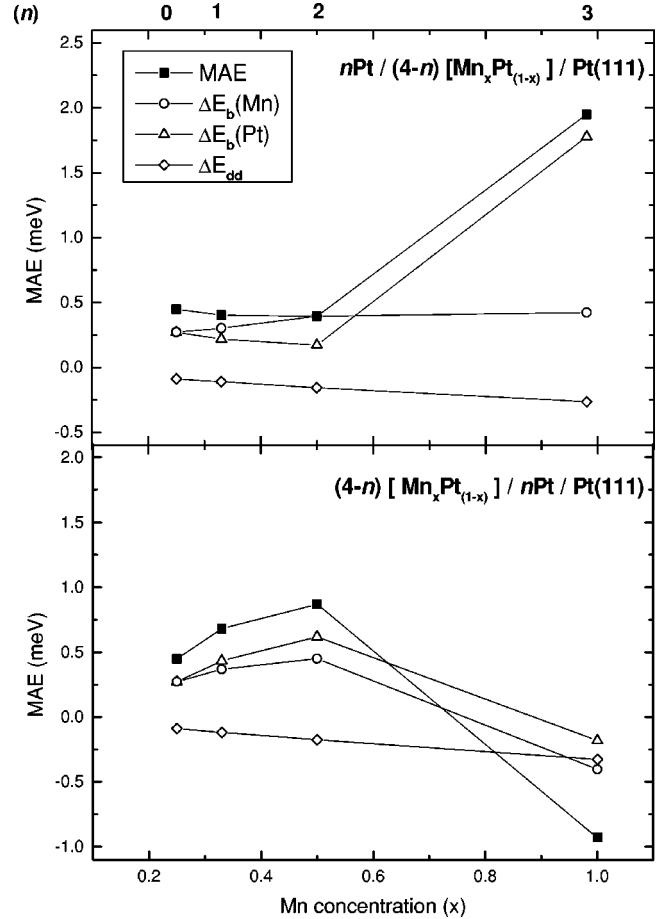


FIG. 2. Same as Fig. 1 for the total magnetic anisotropy energy (MAE). Its decomposition into the chemically resolved band energy (ΔE_b) and the magnetostatic dipole-dipole energy (ΔE_{dd}) is also shown.

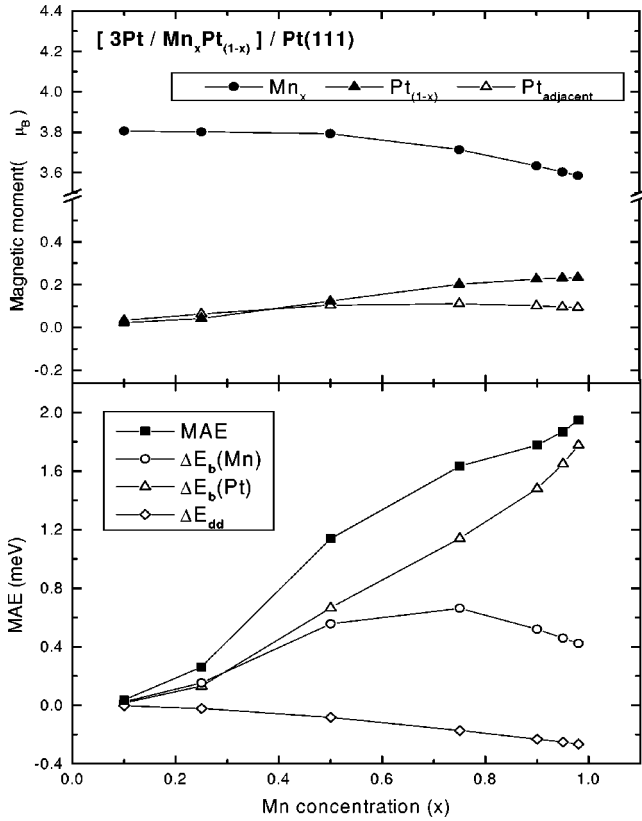


FIG. 3. In the upper panel, we show the evolution with x of the total (spin+orbital) magnetic moments of the Pt and Mn atoms of a $\text{Mn}_x\text{Pt}_{(1-x)}$ layer covered by three Pt planes. For comparison, the Pt moment of one of the adjacent Pt layers is also given. The lower graph corresponds to the evolution of the MAE of the whole surface region, showing also ΔE_b and ΔE_{dd} .

It is interesting to analyze the dependence of the MAE with respect to the interaction between Mn atoms along the (111) direction. In order to do this, we have studied structures formed by a different number of repetitions (n) of a (3Pt/Mn) slab. For comparison, structural sequences $n[\text{Mn}_{0.25}\text{Pt}_{0.75}]$, obtained by the repeated stacking of a single $\text{Mn}_{0.25}\text{Pt}_{0.75}$ plane on Pt(111), have also been considered. In Fig. 4 we show the mean value of the MAE per layer versus n for both kinds of systems. Clearly, it exhibits a saturation with n , which is common to the Mn and Pt band energy contributions. Notice also the strong enhancement of the MAE at the very beginning of the upper graph, corresponding to the 3Pt/Mn slab; this suggests coupling between subsequent magnetic layers separated by a nonmagnetic spacer introducing an increased anisotropy along the normal to the layers. On the other hand, the reduction of the MAE in the lower graph of the figure reflects an isotropic lattice of $\text{Mn}_{0.25}\text{Pt}_{0.75}$ to be associated to larger values of n .

C. Layered $\text{Pt}/\text{Mn}_{0.25}\text{Pt}_{0.75}$ compounds

In the following we will concentrate on those configurations of layered compounds of alternated Pt/Mn-Pt composition closer to that observed experimentally, namely Pt/MnPt_3 , focusing on two main aspects: Pt versus Mn termination, and the chemical ratio in the alloyed planes.

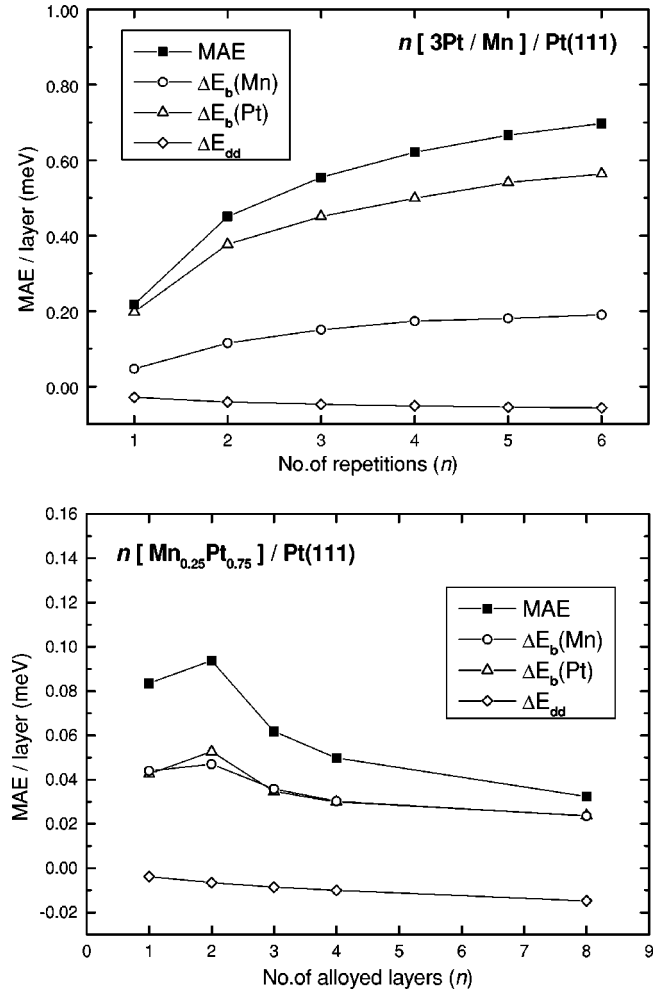


FIG. 4. Dependence on the number of repetitions (n) of the mean MAE per layer for the sequences $n[3\text{Pt}/\text{Mn}]$ (upper graph) and $n[\text{Mn}_{0.25}\text{Pt}_{0.75}]$ (lower graph). The decomposition of the MAE into ΔE_b and ΔE_{dd} is also shown. Notice the different scale of both graphs.

1. Effect of Pt termination

The best way to analyze the effect of a Pt termination on the magnetic properties of layered compounds of alternated plane composition is to compare two identical $\text{Pt}/\text{Mn}_{0.25}\text{Pt}_{0.75}$ sequences, just inverting the relative ordering of the Pt and $\text{Mn}_{0.25}\text{Pt}_{0.75}$ layers. We will also consider the homogeneous surface formed by identical $\text{Mn}_{0.25}\text{Pt}_{0.75}$ layers, which would correspond to the abrupt cut of a chemically disordered MnPt_3 bulk crystal parallel to the (111) plane. The detailed layer structure of these systems, as modeled in our calculations, is described in Table II. Although care should be taken when comparing the total energies of the three structures, due to the different atomic composition of C, it seems that by placing Mn atoms in the layered dispositions, structures A and B are more favorable.

In all surfaces, the magnetic moments of the Mn atoms are $\sim 3.8 \mu_B$, the higher values corresponding to the alternated compositional sequences. They are almost constant in all layers, except for an enhancement of $0.2 \mu_B$ at the top-most plane in structures B and C. The polarization of the Pt

TABLE II. Layer resolved composition of the structures of Sec. III C 1. **A** and **B** refer to the layered Pt/Mn_{0.25}Pt_{0.75} surfaces, and **C** to Mn_{0.25}Pt_{0.75}.

| Structure | A | B | C |
|-----------|---------------------------------------|---------------------------------------|---------------------------------------|
| Layer 0 | Vacuum | Vacuum | Vacuum |
| Layer 1 | Pt | Mn _{0.25} Pt _{0.75} | Mn _{0.25} Pt _{0.75} |
| Layer 2 | Mn _{0.25} Pt _{0.75} | Pt | Mn _{0.25} Pt _{0.75} |
| Layer 3 | Pt | Mn _{0.25} Pt _{0.75} | Mn _{0.25} Pt _{0.75} |
| Layer 4 | Mn _{0.25} Pt _{0.75} | Pt | Mn _{0.25} Pt _{0.75} |
| Layer 5 | Pt | Mn _{0.25} Pt _{0.75} | Mn _{0.25} Pt _{0.75} |
| Layer 6 | Mn _{0.25} Pt _{0.75} | Pt | Mn _{0.25} Pt _{0.75} |
| Layer 7 | Pt | Mn _{0.25} Pt _{0.75} | Mn _{0.25} Pt _{0.75} |
| Layer 8 | Mn _{0.25} Pt _{0.75} | Pt | Mn _{0.25} Pt _{0.75} |
| Layer 9 | Pt | Pt | Pt |
| Layer 10 | Pt | Pt | Pt |
| Layer 11 | Pt | Pt | Pt |
| Layer 12 | Bulk | Bulk | Bulk |

atoms leads to moments of less than $0.1 \mu_B$. In the structures A and B they show an oscillatory behavior, being larger at the planes of pure Pt composition ($\sim 0.09 \mu_B$) than in the Mn_{0.25}Pt_{0.75} planes ($\sim 0.04 \mu_B$).

The MAE of the three systems is compared in Fig. 5. Its positive value indicates that also for the alternated layer compositions, the (111) direction is the preferred axis of magnetization. However, structures A and B show some new features. First, the anisotropy is higher, mainly due to an enhancement of the $\Delta E_b(\text{Mn})$. In addition, there exists a reduction of the absolute value of ΔE_{dd} . On the other hand, if we compare between both structures, we see that a Mn or Pt termination hardly affects the global value of the MAE. A detailed study of the layer-resolved quantities indicates that the only relevant difference can be found for $\Delta E_b(\text{Pt})$ in the two topmost planes: as occurred for the Pt moments, $\Delta E_b(\text{Pt})$ exhibits a bilayer periodicity, adopting negative values in the alloyed planes, while becoming positive in the

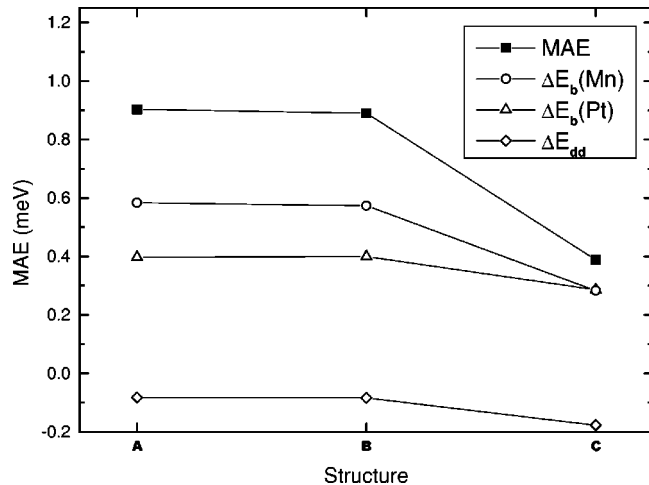


FIG. 5. Comparison between the total MAE of the three structures of Table II, also showing the ΔE_b and ΔE_{dd} contributions.

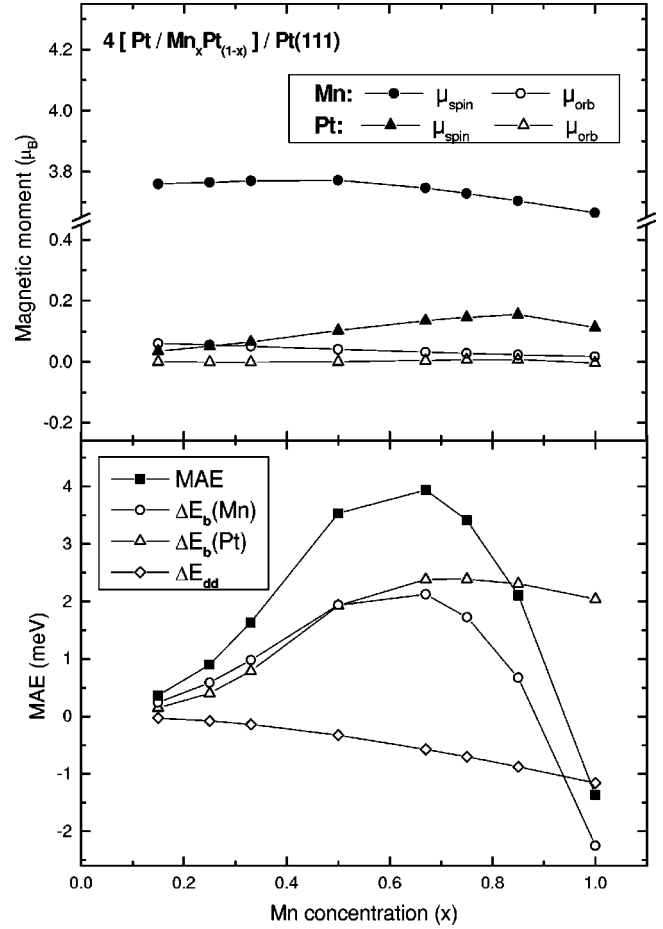


FIG. 6. Evolution with x of the magnetic properties of a layered Pt/Mn_xPt_(1-x) surface, the topmost layer corresponding to a pure Pt plane. The upper panel shows the mean magnetic moments per atom, where the chemically resolved orbital and spin components are plotted separately. The lower graph corresponds to the magnetic anisotropy energy and its decomposition into ΔE_b and ΔE_{dd} .

pure Pt layers; this oscillatory behavior only breaks down at layer one of B, where a positive $\Delta E_b(\text{Pt})$ is found.

2. Effect of Mn concentration

The influence of the Mn concentration on the magnetic properties has been studied by analyzing layered systems Pt/Mn_xPt_(1-x) ($x \in [0,1]$) formed following model A of Table II. Only Pt-ended sequences have been considered, in order to reassemble the experimental stable surface compound, and due to the negligible effect of the termination on the global magnetic properties discussed above.

In the upper panel of Fig. 6 we show the dependence on the Mn content of the component resolved mean magnetic moments in the surface region, defined in Eq. (1). Their variation is small, and the more significant changes correspond to the spin contribution to the magnetic moments.

The MAE of these systems is depicted in the lower graph of Fig. 6. The evolution of the MAE is governed by the band energy contribution, ΔE_{dd} becoming increasingly negative as we add more Mn. The ΔE_b of Mn and Pt follow a similar strong enhancement up to 67% of Mn, which is reflected in

the evolution of the MAE. However, for higher concentrations they show completely different behaviors: while the ΔE_b of Pt remains about constant, that of Mn abruptly decreases, leading even to a change of sign for very high concentrations. As a result, the MAE reduces its value, becoming also negative when we have pure Mn planes in the structure. A further remark can be made. Although the global ΔE_b (Pt) does not follow the strong variation of ΔE_b (Mn) for high x , noticeable changes occur in the layer-resolved ΔE_b (Pt). For low x , it oscillates between positive and negative values in the pure Pt planes and the alloyed ones, respectively. As we increase the amount of Mn, the layer-resolved ΔE_b (Pt) becomes always positive, and for $x \geq 0.67$ it is even higher in the alloyed layers.

IV. DISCUSSION

Although we have studied disordered surfaces, it is interesting to compare them with their ordered counterparts. In principle, different values for the physical magnetic quantities can be obtained for ordered systems. However, in the process of the formation of the stable surface compound (2×2)-[Pt/MnPt₃]/Pt(111) the system undergoes disordered metastable phases before the ordered stoichiometry is achieved. The transition from the disordered to the ordered state develops as a smooth evolution, which can be studied on the basis of the CPA approach. In fact, the reduction of total energy obtained here when the alternated compositional sequence is adopted corresponds to the expected situation associated with a more stable structure. But the existence of compositional order may modify the actual value of the MAE, as has been confirmed for different fcc transition metal films.³ In the case of the ordered bulk MnPt₃ crystal, although the isotropy inherent to the AuCu₃ (L1₂) lattice reduces the MAE,¹⁵ there exists experimental evidence of a slightly preferred magnetization axis perpendicular to (111).⁶ On the other hand, the magnetic moments resulting from our study are in the same range of those obtained at different ordered Mn-Pt surface and bulk systems,^{16–18} that is, values around $3.6 \mu_B$ for Mn and $\sim 0.1–0.2 \mu_B$ for Pt. In particular, the same evolution of the moments from the inner layers to the surface has been determined for the ordered MnPt₃ and Pt/MnPt₃ compounds.¹⁸

From our results, it is evident that the MAE is strongly

influenced by the magnetic environment of the Mn atoms. In addition, it seems that a positive MAE is associated with the layer compositions Mn_{*x*}Pt_(1–*x*) with $x < 1$. The only negative values are found for a Mn overlayer on Pt(111) and for layered Pt/Mn sequences involving pure Mn planes. On the other hand, it is known that a Mn overlayer on a fcc substrate orders antiferromagnetically,¹⁹ which in turn implies that an in-plane coupling other than used in the present paper might also change the size, and even the sign, of the MAE. Presently, our computational scheme is in the process of being extended to the case of complex square lattices,²⁰ which will enable us to deal also with in-plane antiferromagnetic configurations.

V. CONCLUSIONS

We have studied the electronic structure and magnetic properties of chemically disordered surfaces formed by Mn_{*x*}Pt_(1–*x*) planes on top of a Pt(111) substrate. In terms of the reduction of the total energy, favored situations are found when the Mn atoms are completely surrounded by Pt. This leads to Pt-ended surfaces and layered sequences of alternating Pt/Mn_{*x*}Pt_(1–*x*) composition. The Mn spin moments have giant values around $3.8 \mu_B$ in all systems considered. They are enhanced both at the topmost planes and for a larger number of Pt neighbors. The Pt atoms are slightly polarized, with moments $\sim 0.1–0.2 \mu_B$. Especially for the more stable surfaces, the MAE favors a perpendicular magnetization along (111). However, its value depends strongly on the detailed structure and the relative concentration of Pt and Mn.

ACKNOWLEDGMENTS

This work has been partially financed by the Spanish DGICYT (Contract No. PB96-0916) and the Comunidad Autónoma de Madrid (Contract No. 07N/0042/98), and resulted from a collaboration partially funded by the TMR network (Contract No. EMRX-CT96-0089). S.G. thanks support from the Spanish Ministerio de Educación y Cultura. Financial support was also provided by the Center of Computational Materials Science (Contract No. GZ 45.442), the Austrian Science Foundation (Contract Nos. P12146, P12352, and T27-TPH), and the Hungarian National Science Foundation (Contract Nos. OTKA T030240 and T029813).

¹L. M. Falicov *et al.*, *J. Mater. Res.* **5**, 1299 (1990).

²G. H. O. Daalderop, P. J. Kelly, and M. F. H. Schuurmans, *Phys. Rev. B* **44**, 12 054 (1991).

³S. S. A. Razee, J. B. Staunton, B. Ginatempo, F. J. Pinski, and E. Bruno, *Phys. Rev. Lett.* **82**, 5369 (1999).

⁴S. Gallego, C. Ocal, M. C. Muñoz, and F. Soria, *Phys. Rev. B* **56**, 12 139 (1997).

⁵M. Wuttig, Y. Gauthier, and S. Blügel, *Phys. Rev. Lett.* **70**, 3619 (1993); O. Rader, W. Gudat, C. Carbone, E. Vescovo, S. Blügel, R. Kläsches, W. Eberhardt, M. Wuttig, J. Redinger, and F. J. Himpsel, *Phys. Rev. B* **55**, 5404 (1997).

⁶T. Kato *et al.*, *J. Magn. Magn. Mater.* **140-144**, 713 (1995).

⁷R. Zeller, P. H. Dederichs, B. Újfalussy, L. Szunyogh, and P. Weinberger, *Phys. Rev. B* **52**, 8807 (1995).

⁸L. Szunyogh, B. Újfalussy, and P. Weinberger, *Phys. Rev. B* **51**, 9552 (1995); **51**, 12 836 (1995).

⁹P. Weinberger, P. M. Levy, J. Banhart, L. Szunyogh, and B. Újfalussy, *J. Phys.: Condens. Matter* **8**, 7677 (1996).

¹⁰M. Weinert, R. E. Watson, and J. W. Davenport, *Phys. Rev. B* **32**, 2115 (1985); G. H. O. Daalderop, P. J. Kelly, and M. F. H. Schuurmans, *ibid.* **41**, 11 919 (1990).

¹¹L. Szunyogh, B. Újfalussy, and P. Weinberger, *Phys. Rev. B* **51**,

- 9552 (1995).
- ¹²P. Villars and L. D. Calvert, *Pearson's Handbook of Crystallographic Data* (ASM International, Metals Park, OH, 1991).
- ¹³L. Szunyogh, B. Újfalussy, U. Pustogawa, and P. Weinberger, *Phys. Rev. B* **57**, 8838 (1998).
- ¹⁴B. Újfalussy, L. Szunyogh, P. Bruno, and P. Weinberger, *Phys. Rev. Lett.* **77**, 1805 (1996).
- ¹⁵P. M. Oppeneer, V. N. Antonov, T. Kraft, H. Eschrig, A. N. Yaresko, and A. Ya Perlov, *J. Phys.: Condens. Matter* **8**, 5769 (1996).
- ¹⁶B. Antonini, F. Lucari, F. Menzinger, and P. Paoletti, *Phys. Rev. B* **187**, 611 (1969).
- ¹⁷A. Hasegawa, *J. Phys. Soc. Jpn.* **54**, 1477 (1985).
- ¹⁸S. Gallego, L. Chico, and M. C. Muñoz, *Phys. Rev. B* **57**, 4863 (1998).
- ¹⁹T. Asada, G. Bihlmayer, S. Handschuch, S. Heinze, P. Kurz, and S. Blügel, *J. Phys.: Condens. Matter* **11**, 9347 (1999); **57**, 4863 (1998).
- ²⁰C. Uiberacker, L. Szunyogh, B. Újfalussy, and P. Weinberger, *Philos. Mag. B* **78**, 423 (1998).